NASA TECHNICAL NOTE

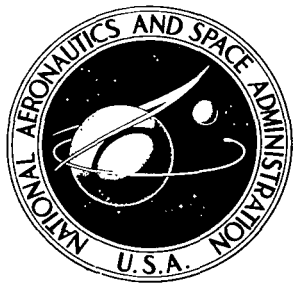

THE ORBITING ASTRONOMICAL OBSERVATORY THERMAL TEST PROGRAM

by
P. Caruso, Jr., C. Dan, Jr., and E. Young
Goddard Space Flight Center
and
D. Mengers
Grumman Aerospace Corporation

NATIONAL AERONAUTICS AND SPACE ADMINISTRATION • WASHINGTON, D. C. • AUGUST 1970

1. Report No.	2. Government Accession No.	3. Recipient's Catalog No.
NASA TN D-5794		

4. Title and Subtitle
The Orbiting Astronomical Observatory Thermal Test Program

5. Report Date
August 1970

6. Performing Organization Code

7. Author(s) P. Caruso, Jr., C. Dan, Jr., E. Young, and D. Mengers

8. Performing Organization Report No.
G-963

9. Performing Organization Name and Address
Goddard Space Flight Center
Greenbelt, Maryland 20771

10. Work Unit No.
831-31-25-01-51

11. Contract or Grant No.

12. Sponsoring Agency Name and Address
National Aeronautics and Space Administration
Washington, D.C. 20546

13. Type of Report and Period Covered
Technical Note

14. Sponsoring Agency Code

15. Supplementary Notes

16. Abstract

The Orbiting Astronomical Observatory (OAO) 2 was successfully launched on December 7, 1968. The purpose of the mission was twofold: (1) to provide a stabilized platform for astronomical observations in the ultraviolet; and (2) to yield survey information to assist in design of future astronomical experiments. Prior to launch, the OAO was subjected to a rigorous development program of test and analysis. Observatory thermal testing was conducted at Goddard Space Flight Center. The thermal test and evaluation program consisted of an Alzark heater skin thermal balance study, a radiation model test, a solar array test, several thermal balance and electronic functional tests on the spacecraft experiment packages, a thermal model test, and two combined thermal vacuum electrical functional checks on the integrated spacecraft. The significant results of the test program, a review of the thermal evaluation methods employed, and the problems encountered in assessing the Observatory thermal performance are presented.

17. Key Words Suggested by Author	18. Distribution Statement
OAO 2 Test Thermal Test	Unclassified--Unlimited

19. Security Classif. (of this report)	20. Security Classif. (of this page)	21. No. of Pages	22. Price *
Unclassified	Unclassified	40	$3.00

*For sale by the Clearinghouse for Federal Scientific and Technical Information Springfield, Virginia 22151

CONTENTS

THE ORBITING ASTRONOMICAL OBSERVATORY THERMAL TEST PROGRAM

by

P. Caruso, Jr., C. Dan, Jr., E. Young
Goddard Space Flight Center

and

D. Mengers
Grumman Aerospace Corp.

INTRODUCTION

The Orbiting Astronomical Observatory (OAO) 2 was successfully launched on December 7, 1968, into a near-circular orbit by a two-stage Atlas/Centaur rocket. The OAO 2 (Figure 1) is the second of a series of spacecraft being developed for Goddard Space Flight Center by the Grumman Aerospace Corp. to advance man's knowledge of the origin and development of the universe by long duration astronomical observations above the Earth's atmosphere (Reference 1). OAO 2 contains two onboard experiments. One, the Smithsonian Astrophysical Observatory (SAO) experiment, has as its prime objective a survey of the sky in the ultraviolet portion of the spectrum. The other, the Wisconsin experiment package (WEP), is a broad band photometry experiment (Reference 1).

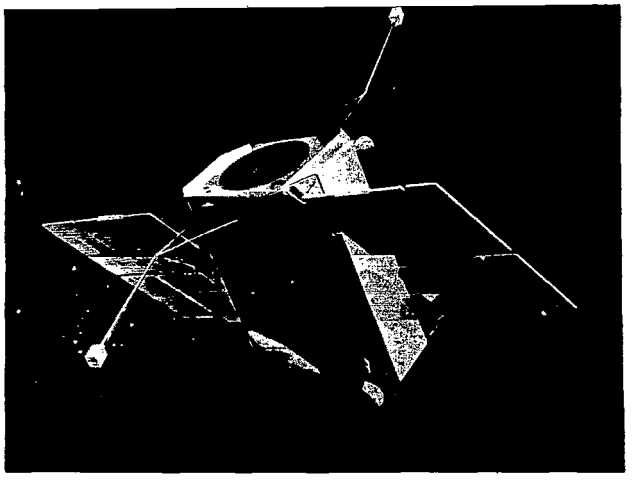

Figure 1—Artist's conception of OAO 2.

OAO 2, the largest and most complex unmanned scientific satellite to be tested at Goddard, was constructed with an octagonal main body, 80 in. across the flats, 116 in. high, and approximately 4,400 lb in weight.

Located within a 48 in. diameter central tube, the two onboard experiments, the WEP (Figure 2) and the SAO (Figure 3), could view the stellar sphere from opposite ends of the spacecraft.

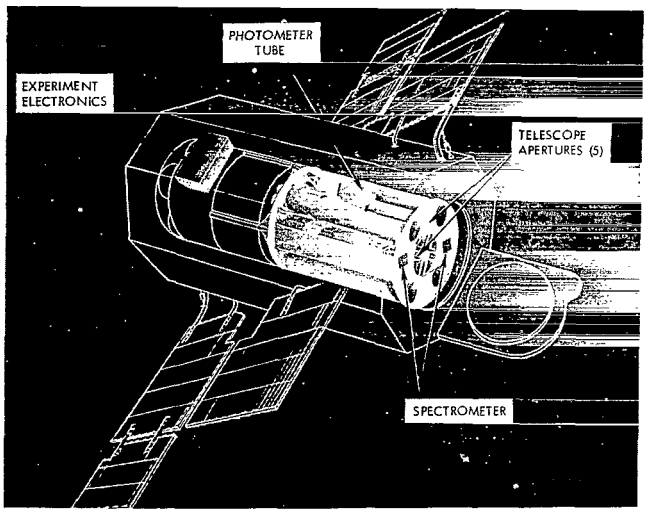

Figure 2—The Wisconsin experiment package.

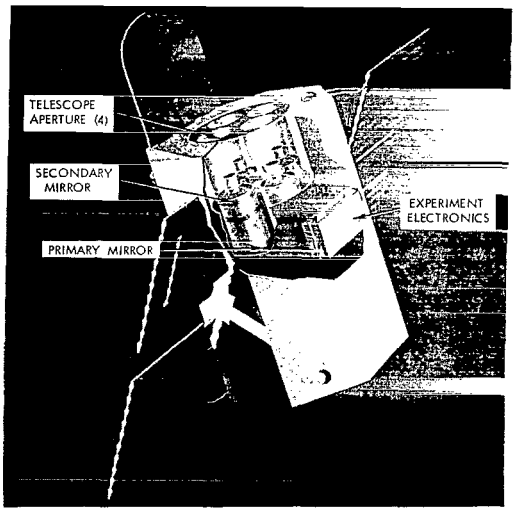

Figure 3—The Smithsonian Astrophysical Observatory experiment.

The support equipment, which included the power, data, communications, and stability and control subsystems, was mounted on either aluminum or honeycomb heat sinks located in 48 insulated bays surrounding the central tube. The external surfaces, including the forward and aft ends of the spacecraft, were covered with Alzak* skins to afford passive thermal control. The side and level of a bay along a side were identified using an alphanumeric designation, A-H for the eight sides and 1-6 for the bay level along the side (Figure 4).

Eight solar paddles (Figure 5), covered on both sides with *N/P*-type cells, supplied power to the spacecraft and charged the three onboard nickel-cadmium batteries. The solar paddles were erected perpendicular to the C and G sides at an angle of 33° to the optical axis.

Two controllable aperture covers (sunshades) protected the experiments from direct sunlight. The surface facing the experiment aperture was black; the other surface was covered with Alzak sheeting.

Because of the OAO requirements for reliable design performance, a detailed program of thermal testing and evaluation was mandatory. This paper presents the

*Alzak is an Alcoa material consisting of a base sheet of 3003 series aluminum, which is clad on one side with 99.87% pure aluminum. The clad side is then electropolished and clear anodized with an aluminum oxide coating thickness of 0.15-0.25 mil (Reference 2).

significant results of the test program, the thermal evaluation methods employed, and the problems encountered in the assessment of the OAO 2 thermal performance.

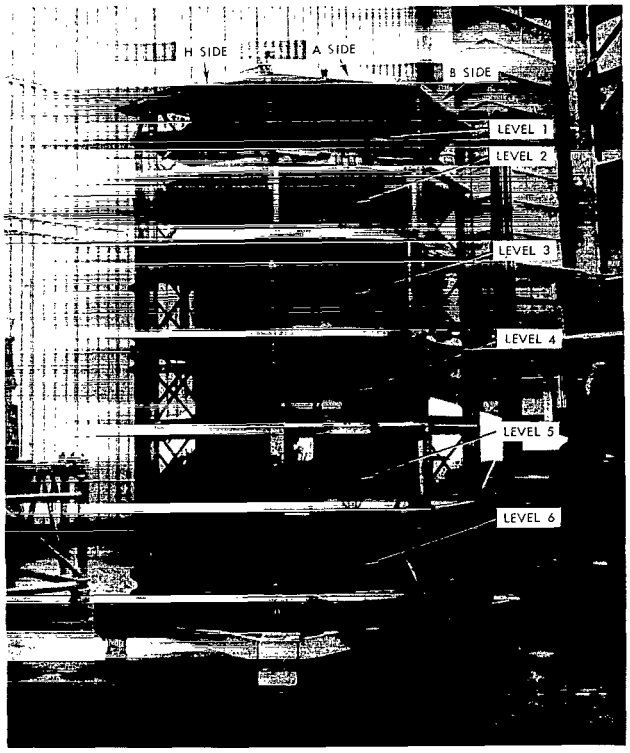

Figure 4—OAO 2 bare structure.

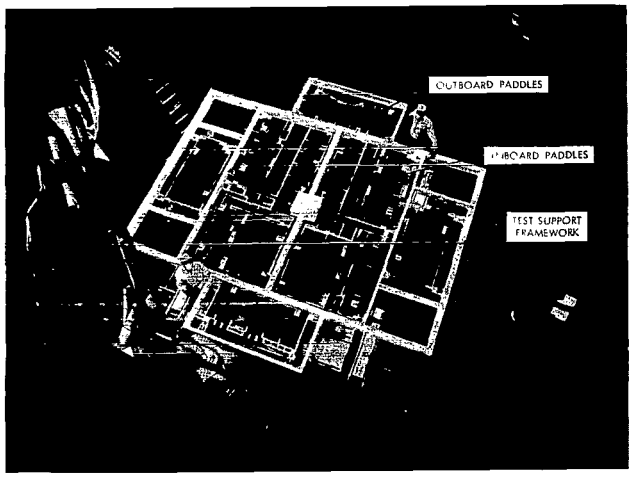

Figure 5—OAO 2 solar paddles.

THERMAL DESIGN

The spacecraft was designed for a nominal circular orbit of 500 statute miles with an inclination of 35° to the Equator. As the orbit precesses about the Earth, the OAO can be in sunlight from 65% to 83% of one orbit.

Two orientation angles are used to describe the orbital position of the OAO (Reference 3): β and γ. Angle β is the angle between a line parallel to the Earth-Sun line and the optical axis of the spacecraft. Angle γ is the angle between two planes, one determined by the optical axis of the spacecraft and a line parallel to the Earth-Sun line and intersecting the optical axis, the other determined by the Earth-Sun line and the north ecliptic pole. When $\beta = 0°$, the forward end is pointing away from the Sun. If $\beta < 90°$, the A, B, and H sides and the aft end receive sunlight. When $\beta > 90°$, the D, E, and F sides and the forward end are in sunlight.

The A, E, forward, and aft skins can be oriented anywhere from no sun to sun normal to the surface. The B, D, F, and H skins can experience any range from no sun to sun at a 45° angle to the surface. The C and G sides are kept parallel to the Sun's rays so that the solar paddles are not shadowed.

Spacecraft thermal control was accomplished by the use of active elements (heaters and louvers) and passive thermal skins.

Alzak sheeting was chosen for the outer spacecraft skins because of the low ratio of solar absorptivity ($\alpha = 0.15$) to total hemispherical emissivity ($\epsilon = 0.75$).

Because of a wide range of power dissipations in various bays, a number of the bays included active thermal control elements (Figure 6). These bays were designed to stay below the hot temperature limit, but additional heater power was provided to maintain equipment above the cold limit. Where used, heaters were controlled by thermostats set approximately 5°C above the cold temperature acceptance limits. So that power demands for thermal control could be minimized, these same bays were also evaluated to determine if thermal louvers could be employed. The louvers used for OAO 2 were polished aluminum blades held on a frame that was mounted between the heat sink and side skin. The blades were attached to bimetallic springs that sensed the heat sink temperature. As the temperature increases, the springs open the blades and expose more of the black heat sink. As the temperature drops, the blades close and provide a polished aluminum shield between the heat sink and skin.

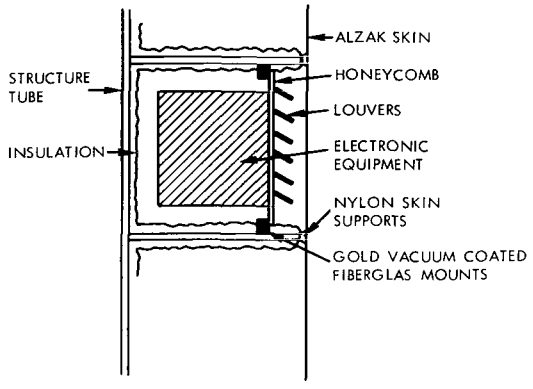

Figure 6—OAO 2 equipment bay design.

Several pieces of equipment dissipated so much power that the physical size of the bays was too small to reject all the heat, even with an all-black heat sink. In these cases, the insulation was removed from the structure to allow the equipment to radiate heat to the structure. Also, structure bays on levels 1, 2, and 6 on the C side and on levels 1, 2, 5, and 6 on the G side had insulation removed so that they could be used as cooling bays to control the heat leak from the structure to space.

In the final configuration, there were 30 equipment bays, five of which had louvers, 16 of which had heaters, and three of which radiated to structure. Four of the five louvered bays had heaters, and three of these radiated to the structure.

Each major subdivision of the spacecraft had different temperature constraints. Specifically, the spacecraft structure temperature range was limited to $-18° \pm 22°C$. Most electronic equipment heat sink temperatures were restricted to an interval of $-18°$ to $+54°C$. The WEP and the SAO experiment electronics were designed to operate above $-49°C$ and below room temperature. The lower bounds on the optical mirrors of the WEP and SAO were $-52°C$ and $-65°C$, respectively. In addition, experiment heat leaks were to be minimized.

ENVIRONMENTAL TEST FACILITY

The integrated testing of the Observatory was performed at GSFC in the Space Environmental Simulator (SES). See Figures 7 and 8 for chamber details.

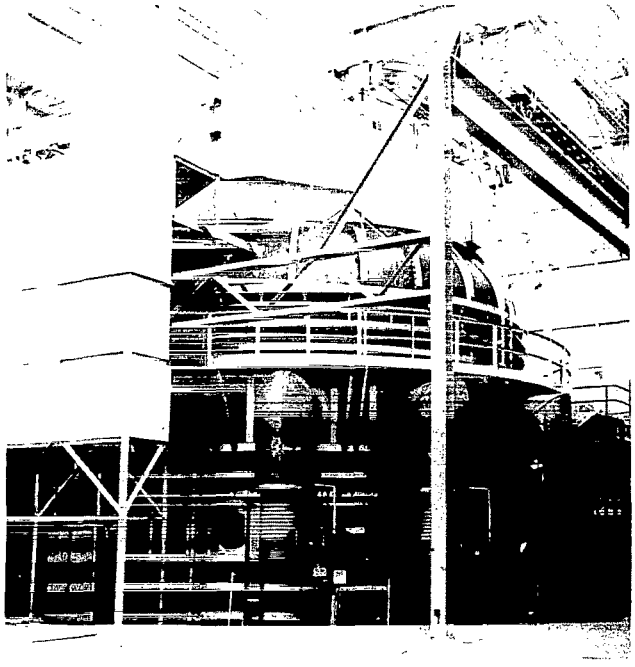

Figure 7—The Space Environmental Simulator.

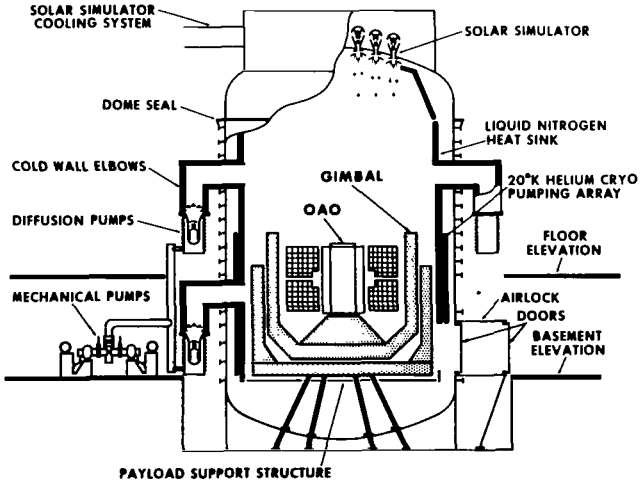

Figure 8—Details of the Space Environmental Simulator.

The SES is a large solar vacuum test chamber. The chamber contains a heat sink system, a vacuum system, a solar simulator, and a single-axis spacecraft positioner (gimbal). The SES is also equipped with contamination control facilities, a data acquisition system, and an emergency power system.

Liquid nitrogen is circulated through the black tube-in-sheet aluminum paneling that makes up the inner curtain wall of the chamber. Except for the artificial sun in the dome, this wall shrouds the entire inside of the chamber and its cryogenic pumping system.

A combination of eight mechanical booster pumps and 17 oil diffusion pumps, augmented when required with a dense gas helium cryopump system, creates the low-level pressure to simulate the vacuum environment of space. The vacuum system can reduce the ultimate pressure of the 33 ft diameter, 58 ft high, stainless steel chamber to 1×10^{-8} torr in 18 hours.

The solar simulator consists of 127 optical modules forming a hexagonal array in the dome of the chamber. This array projects its light to the chamber floor over a 20 ft hexagonal pattern. The intensity of the solar beam can be varied from 80 to 150 W/ft^2 with a decollimation half-angle of 2°.

In order to sample the solar beam in test, the SES is equipped with two scanners composed of 84 solar cells. The solar cells are calibrated against NBS standard lamps in a separate facility and against total energy radiometers mounted on the scanner. The intensities measured by these solar cells are recorded and processed by a high-speed data system to provide statistical data of the intensity at the scan elevation.

Within the chamber, a gimbal orients the test vehicle with respect to the solar simulator. The design includes two U-frames with a motor drive to position the movable inner frame from 90° on one side of the vertical plane to 120° on the other side. Eight adiabatic interfaces at the spacecraft mounting points prevent heat transfer between the movable U-frame and the spacecraft. All surfaces facing the spacecraft are LN_2 cooled.

The chamber is equipped with an air conditioning system to control particulate contamination. A clean room environment of class 10,000 or better is achievable. Supply air is filtered and maintained at 21°±2°C with a relative humidity of 40% to 45%.

The data acquisition system for the Goddard facilities consists of a centralized data collection system and four computers. The prime purpose of the on-line computer system is collection, processing, and display on demand of selected data from both facility and spacecraft during environmental testing. Input data to the system (2500 channels sampled every 100 seconds) are converted to engineering units and read out at the chamber.

In the event of a power failure, the associated emergency control equipment switches the electrical load automatically to the emergency power system. Power is furnished from a diesel-driven generator, which could supply 500 kW continuously or 600 kW for 24-hour operation.

THERMAL TEST PROGRAM

The objectives of the OAO Thermal Test Program were to provide maximum confidence in the total Observatory operability in the thermal-vacuum environment and to evaluate the Observatory thermal performance.

Essentially, two factors controlled the approach taken to implement the test objectives, namely, the status of the Observatory design and the test facility constraints.

The need for a preflight unit became apparent early in the test program planning (Reference 4). It was decided that a thermal model be built to evaluate the suitability of the Observatory thermal design and of proposed thermal design changes, and to provide a test bed for new or redesigned subsystems before the flight unit test.

The chamber in which the thermal testing was to be performed had several significant constraints. Although the solar simulator was capable of illuminating the entire Observatory body and the unfolded inboard solar arrays, the outboard arrays fell outside the solar beam, which precluded a complete thermal and functional test of the Observatory. The fact that the SES was not capable of simulating either albedo or earth infrared radiation imposed additional testing constraints. Since, in the case of OAO 2, these thermal inputs represented 50% of the energy absorbed in certain aspect angles, the albedo and earth infrared radiation had to be included in the thermal simulation.

The constraints caused by size limitations were circumvented by simulating inputs to the spacecraft from appendages (booms, outboard arrays, SAO sunshade) with heaters at the proper spacecraft location. Finally, all external energy inputs were accounted for by use of Alzak heater skins initially developed by Grumman Aerospace Corp. to test OAO 1.

As in all environmental test programs, it was necessary to devise additional tests to provide certain baseline thermal measurements. Since the Observatory solar array and sunshades could not be accommodated in the SES, Observatory tests and thermal model tests had to be performed without these items. Thus, a need arose to measure spacecraft-to-paddle and spacecraft-to-sunshade flux interchange (direct and reflected).

Additionally, there was a need to define any simulation errors caused by heater skins used as flux input devices or caused by stray radiation within the SES chamber. Hence, the need for a heater skin test and a chamber calibration test.

The complete OAO/SES test program consisted of —

(1) Solar calibration test.
(2) Integrating sphere test.
(3) Alzak heater skin test.
(4) Detector model test.
(5) Thermal model test.
(6) Solar array test.
(7) Flight unit test.

A major change in the test program occurred shortly after the delivery of the spacecraft for integration and test. Due to the amount of modification to the basic spacecraft design, the project management decided to run a thermal-vacuum test on the entire Observatory as soon as integration was completed. The purpose of the test was to uncover at the earliest possible time any major flaws in the Observatory system design. The net result on the Thermal Test Program was the addition of a prototype test at acceptance test levels, called the early thermal-vacuum test (ETV). the flight acceptance test was then called the late thermal-vacuum test (LTV).

TEST RESULTS

Solar Calibration Test

As outlined in the previous section, the thermal test program began with two SES calibration tests. The first of these tests was planned to determine the volumetric intensity and uniformity profile of the solar beam.

During the solar calibration test, intensity and uniformity were measured at levels of 26 and 33.5 ft below the chamber lamps for nominal intensities of 1.0, 0.83, and 0.65 solar constant (Reference 5). Test results showed that the variation in intensity was more than the desired ±10% across the solar beam.

Integrating Sphere Test

The second calibration test (integrating sphere test) was used to cross-check the solar cell intensity data and to measure total chamber infrared energy input to a test volume by allowing a 36 in. diameter black sphere of known surface properties to reach a stabilization temperature in a cold, hard vacuum with the lamps on and then off. The

sphere was located at the geometric center of the test volume to be occupied by the OAO spacecraft and was conductively isolated from the chamber walls.

Test results verified the solar cell intensity data and also showed that reflections and emitted energy from the gimbal were negligible with the lamp system on. In addition, the stray infrared energy into the test sphere was determined to be approximately 14 W (Reference 6).

Alzak Heater Skin Test

The Alzak heater skin thermal balance test measured the absorptivity-emissivity ratio (α/ϵ) of the test skins and of several control samples. Also, a baseline check of simulation techniques necessary for the detector model and thermal model tests would be obtained by driving the Alzak skins to stabilization under heater power ($i^2 R$) with lamps off and comparing this power with the solar absorbed power ($IA\alpha$) needed to bring the Alzak skins to the same temperature. The ratio ($i^2R/IA\alpha$) was then to be used in determining a correlation factor to be used when heater power was substituted for solar simulation in subsequent OAO detector and thermal model tests.

The α/ϵ ratio of the heater skins and control samples was determined experimentally by locating the test items normal to the mercury-xenon beam in the SES facility (Figure 9). The skins and samples, insulated on the anti-solar side with aluminized Mylar, were mounted to a support rack constructed in such a way that eight Observatory side skins and 20 control samples could be suspended between its structural members. The forward skin of the Observatory rested on Teflon-insulated aluminum angle beams. Because of chamber size limitation, only nine of 26 heater skins were tested, with Student's t distribution used to obtain a representative sampling.

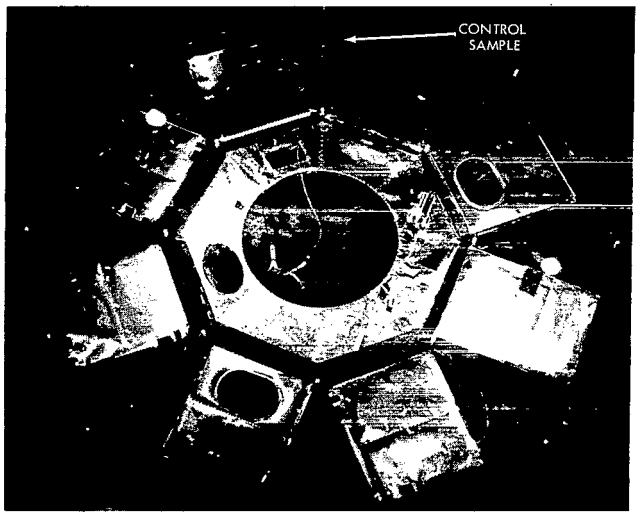

Figure 9—The Alzak heater skins in test configuration.

The α/ϵ ratio for each skin and sample was calculated by monitoring stabilization temperatures, incident solar intensity on each test item, insulation temperatures, chamber wall temperature, and physical data peculiar to each test item. From the collected data, α/ϵ, α, ϵ, and the uncertainties of measurement associated with each quantity were computed for each heater skin. The standard thermal balance equations used included the effects of lamp and infrared inputs, decollimation, and insulation, edge, and conductive losses. The α/ϵ values were also calculated for each Alzak sample. The results were as follows:

(1) The ratio α/ϵ varied significantly with solar time. Since ϵ was relatively fixed with time, degradation in α accounted for the change in α/ϵ. The rate of degradation was approximately 1% per solar day.

(2) The forward skin was found to be severely degraded after test, the Alzak thickness of the degraded areas being approximately 0.06 mil. It was judged that the thickness value (out of tolerance) explained the severe degradation problem.

(3) The α/ϵ values calculated for each control sample showed a great deal of scatter and hence were not reliable data. The fault was linked to difficulties in measuring intensity over each small sample area, in mounting small samples in the large chamber, and in insulating the small test specimens.

(4) Because of significant degradation of α with time under solar vacuum, a constant correlation factor $(i^2R/IA\alpha)$ was an impossibility.

Detector Model Test

Before the thermal model test, a detector model test* was conducted to—

(1) Confirm the coupling factors from the solar arrays to the spacecraft and from the forward sunshade to the spacecraft.

(2) Determine the effective conductance (K/L) of the sunshade.

(3) Further investigate the Alzak skin thermophysical properties.

To attain these objectives, the test configuration included a structural model of the Observatory (Figure 4), Alzak heater skins, a modified experiment sunshade, dummy solar arrays simulating the four inboard paddles, and black plate monitoring sensors (on the C bays, on the forward end of the spacecraft, and on the experiment aperture).

The scheduled test program was divided into several phases. In the first phase, the solar arrays were controlled to expected flight temperatures, including lateral gradients, and the input to the spacecraft was measured. In the second phase, the sunshade was temperature controlled to flight levels, and the thermal input to the forward-end skin sections was measured. At this time, the sunshade conductance was also determined. As an additional output, the emissivity versus temperature of the Alzak heater skins was sampled.

Test results showed a 20% flux increase into battery bay C-4 over that predicted by analysis. This difference, the maximum that occurred between theoretical and experimental test fluxes from the arrays to the spacecraft, was due to the fact that the edges of the Alzak heater skins (approximately 10% of the skin surface area) were not considered in the analysis.

*Hunter, J., "Detector Model Test Report," Thermodynamics Branch, Goddard Space Flight Center, Nov. 1967, unpublished.

Compared with flight predictions, the test fluxes showed a maximum difference of 10% in the C-1 and C-2 bays. The discrepancy was attributed to the fact that the test arrays were maintained at an average temperature, whereas the flight arrays were known to support a significant transverse gradient from the solar to the anti-solar sides.

The tests on the paddles, where lateral gradients were and were not simulated, resulted in a flux difference to the spacecraft of less than 3%. The small difference implied that the fluxe were more dependent on total inputs than on gradients due to spacecraft reflections.

The sunshade couplings to the forward-end skin were determined analytically and the findings confirmed by test. The sunshade conductance (K/L) was calculated to be 10.0 Btu/hr ft^2 °R; the test determined value was 7.5 Btu/hr ft^2 °R.

The Alzak skin emissivity-temperature effects were studied by powering the skins and monitoring the corresponding stabilization temperature. The nominal emissivity was shown to vary from 0.60 to 0.75 for a corresponding temperature range of -104°C to -7°C (Figure 10).

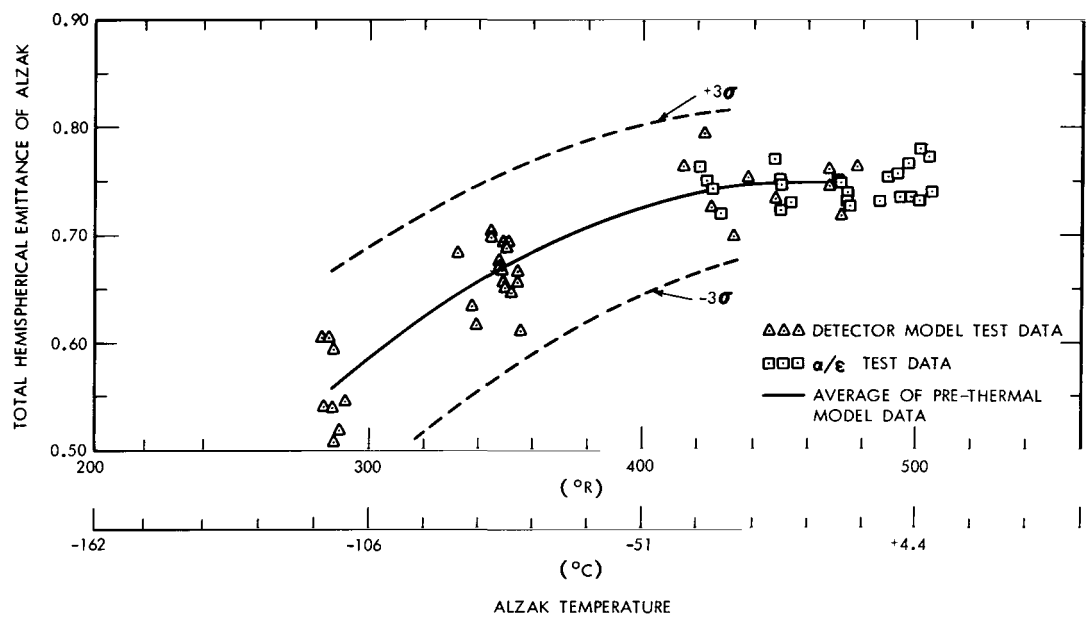

Figure 10—Emissivity of Alzak versus temperature.

The combined results of the detector model and Alzak heater skin tests showed high degradation rates and greater Alzak sensitivity to chamber infrared inputs than was expected under solar vacuum. Because of these findings, all speculation about using the solar simulator in conjunction with heater skins for the Observatory test was dropped. Planning proceeded in the direction of inducing equivalent solar, Earth reflected, and Earth emitted fluxes with the heater skins only.

Thermal Model Test

The thermal model test, lasting 42 days, was performed to determine any design changes necessary for proper thermal control of the flight spacecraft and to verify the analytical model used to generate flight predictions. The thermal model (Figure 11) was configured as closely as possible to the actual spacecraft. Certain equipment (solar paddles, sunshades, and booms) was excluded from the test configuration because of the results of earlier testing.

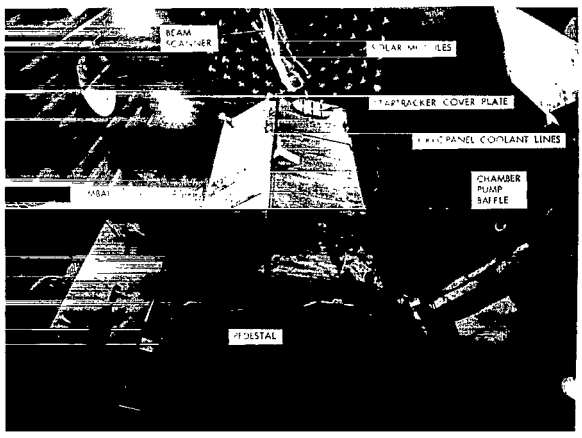

Figure 11—The thermal model of OAO 2.

Though attention to component details provided reasonable simulation, the model was electronically "inert." All bay components were simulated by boxes with internal resistance-type heaters. These dummy packages were the same as the flight model equipment in size, weight, coating, and in the electronic heat dissipation. The various boxes were mounted to the heat sink in the same manner as the live electronics would be mounted for the flight Observatory (Figure 12).

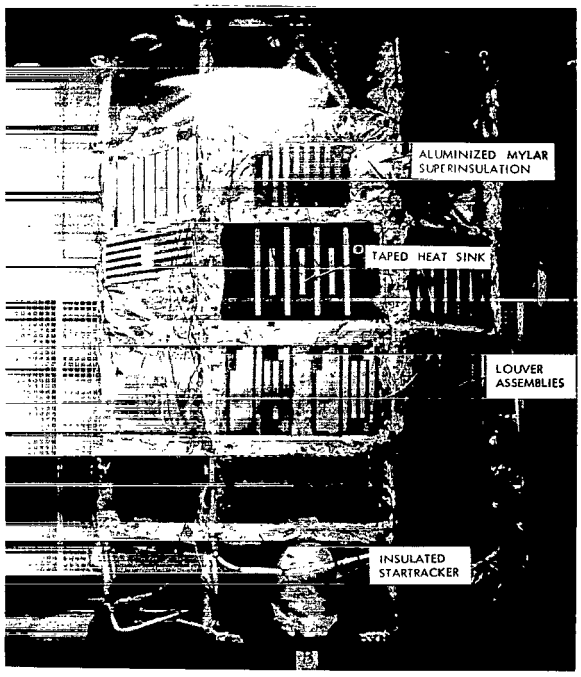

Figure 12—The thermal model with skins removed.

Of the active thermal control elements, only the louvers were included in the configuration in all areas except bay E-1. Instead, the E-1 heat sink was taped to represent the louver's full-open position. The thermal effects of the heaters were simulated by power adjustments of the equipment heaters.

Only one prototype of the six flight startrackers (located in bay H-6) was installed in the model (Figure 13), the other units being thermal mockups without the minaret assemblies. Startracker power was simulated by power resistors on the electronics baseplate. Because the dummy startrackers were completely surrounded with aluminized Mylar blankets, thermal balance information could not be obtained.

The WEP was a working prototype and the SAO was a flight unit replica, except for one thermal dummy telescope. A 47 in. diameter cryopanel provided the effective aperture flux conditions and a method of measuring the experiment heat leak.

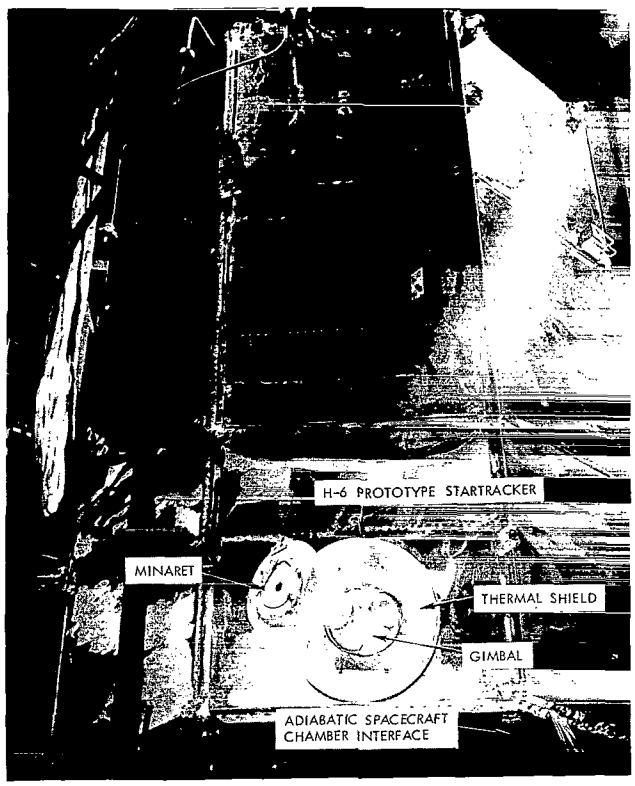

Figure 13—Startracker configuration during thermal model test.

The test was divided into various phases: (1) the Standard Temperature Pressure test to simulate the on-pad functional checkout period, in order to determine the temperature levels of various components; (2) an orbital operations check to study component temperature response at launch power conditions; (3) thermal stabilization checks at several aspects to obtain steady-state temperature data; and (4) a series of special tests to study spacecraft-chamber interfaces, the prototype startracker, bay F-5, and bay D-6.

For the entire test, Alzak heater skins simulated the absorbed environmental fluxes, except for two brief solar simulation tests on the prototype startrackers. Tolerances and uncertainties, added to the environmental fluxes, accounted for worst-case conditions.

The results of the simulated launch pad operations were later used during the various spacecraft ambient checks as a guide to allowable times of component operation.

The simulated orbital operations run established the Observatory operations procedure for the first several hours in flight. No temperature problems or lack of available heater capacity were indicated. Further, the thermostatically controlled heaters were found to be adequate for holding the spacecraft temperatures well above the cold temperature acceptance limits in the first cold case ($\beta = 0°$) check.

The stabilization tests at $\beta = 123°$, 90°A, ($\beta = 90°$, with A side receiving sunlight), 90°E, ($\beta = 90°$, with E side receiving sunlight), 0°, and 0° and 90°A with 2σ tolerances (conservative cold and hot case) uncovered six equipment bays that required design modifications to insure proper thermal control. Heat sink tape patterns and insulation schemes were changed for these bays. Also, the experiment and light seal end losses were higher than predicted but of the same magnitude as those found in the experiment subsystem acceptance test. Test data revealed no significant thermal problems for the WEP and SAO experiments. However, the unresponsive thermostatically controlled heaters in the WEP needed correction.

To validate the use of 2σ flux values averaged for the expected orbit, and to provide additional design information, transient heat fluxes were imposed on bay F-5, chosen because control of the gyro temperature was critical. The test confirmed the design and established the adequacy of the orbital average input approach.

The results of the abbreviated D-6 bay test indicated that the special heater buried in the instrumentation cable bundle minimized the cable heat leaks from the thermal model.

Twice during the test program, solar illumination was used on the H-6 bay prototype startracker to determine the component temperatures. Before testing, an analog computer model for the startracker was developed, and test predictions were generated. The test data and temperature predictions are compared in Table 1.

Table 1—H-6 prototype startracker temperature comparisons.

Test conditions			Test temp. (° C)				Predicted temp. (° C)		
Aspect Angle	Simulation	Power*(W)	Structure	Skin	Minaret	Telescope housing	Telescope	Minaret	Telescope housing
0°	Heater	5.5	-28.7	-70.9	-112.8	- 4.8	- 8.2	- 93.2	- 7.1
0°	Solar	3.8	-25.9	-58.7	- 43.2	- 5.4 ↑	- 9.8	- 36.5	- 9.3
0° (2σ)	Heater	4.6	-33.2	-79.3	-120.0	-19.6	-18.2	-100.6	-17.6
30°	Heater	4.8	-16.6	-40.9	-102.2	- 6.5	- 9.3	- 75.4	- 8.2
90° A	Heater	9.2	- 9.8	- 6.5	...	33.0	27.4	- 46.5	34.6
90° A (2σ)	Heater	8.4	35.7	3.0	- 77.2	32.4	25.2	- 40.4	26.3
90° A (2σ)	Solar	2.0	11.3	7.7	1.3	40.2 ↑	26.8	9.6	27.4
123°	Heater	4.7	-11.5	-68.7	...	- 5.9	-12.1	- 92.6	-10.9

*Input to electronics and base plate

As pointed out in the discussion of the thermal model, the experiment heat leak was measured by using calibrated cryopanels as calorimetric monitoring panels. The results are given in Table 2.

Table 2—Experiment heat leaks.

Aspect angle β	Experiment	Experiment heat leak (W)	
		Calculated	Measured
123°	WEP	40.3	41.0
	SAO	10.7	6.0
90° E	WEP	47.9	44.0
	SAO	6.1	1.0
0°	WEP	6.3	4.0
	SAO	- 3.0*	-16.0
0° (2σ)	WEP	38.5	40.0
	SAO	-11.0*	-19.0
30°	WEP	40.5	45.0
	SAO	6.6	- 5.0

*Negative value indicates heat gain.

Solar Array Test

The 10 flight solar arrays (Figure 5) were subjected to both a thermal cycling test and an array performance check.

The test hardware was designed so that the solar paddles, thermally isolated by nylon standoffs from the support work, could be rotated in the solar beam to irradiate both sides of the arrays. Positioned directly beneath the arrays was a Nichrome grid wire heater to simulate the Earth, albedo, and spacecraft-reflected inputs to the anti-solar side of the paddles. The spacecraft was simulated in test by a resistor load box connected to the array output.

The results of the cycling tests revealed no significant damage to the arrays. Of a total of 105,000 solar cells, approximately 100 were destroyed. The tests did reveal, however, that the flight thermistors were inadequate because of their 85 second time delay. Further, the thermistors were nonlinear outside the range -24° to +40°C.

Determination of the thermal and electrical characteristics during the steady state runs was not possible for the following reasons:

(1) The intensity profile could not be resolved precisely enough, and solar beam nonuniformities (greater than ±10%) were too large.

(2) The lateral and transverse conductance of the solar array composite was not accurately known and could not be determined in test.

(3) The solar cell electrical conversion efficiency was not established for the mercury-xenon spectrum.

It was noted, however, that the pre- and post-test current-voltage measurements did not reveal any significant permanent changes as a result of the test. This fact implied that solar cell ultraviolet degradation was not experienced.

Flight Unit Testing

Imposition of the thermal extremes on all spacecraft systems implies a hot and a cold condition, i.e., two test runs. Such is not the case with the OAO, which can operate with either the A or the E side in full sunlight. The full gamut of test conditions for OAO 2 is outlined below:

Orientation	Condition imposed
$\beta = 90°$ A	Hot structure, hot equipment in bays A, B, and H, hot WEP
$\beta = 90°$ E	Hot structure, hot equipment in bays D, E, and F, hot SAO
$\beta = 0°$ or 180°	Cold structure, cold equipment

Orientation (Cont.)	Condition imposed (Cont.)
$\beta = 123°$	Hot equipment in C and G bays
$\beta = 30°$	Cold WEP
$\beta = 150°$	Cold SAO

In both flight tests, the Observatory (Figure 14) contained the full complement of equipment. In the ETV test, several components were nonflight units, notably startrackers and batteries; in the LTV test, all equipment was flight. The test configurations, however, did not contain solar arrays, booms, sunshades, startracker minarets, and flight skins. Test additions included cryopanels covering both the WEP and SAO optics, Alzak heater skins, light sources hard-mounted directly to solar sensor optics, and a continuous N_2 fill and dump for the pneumatics systems.

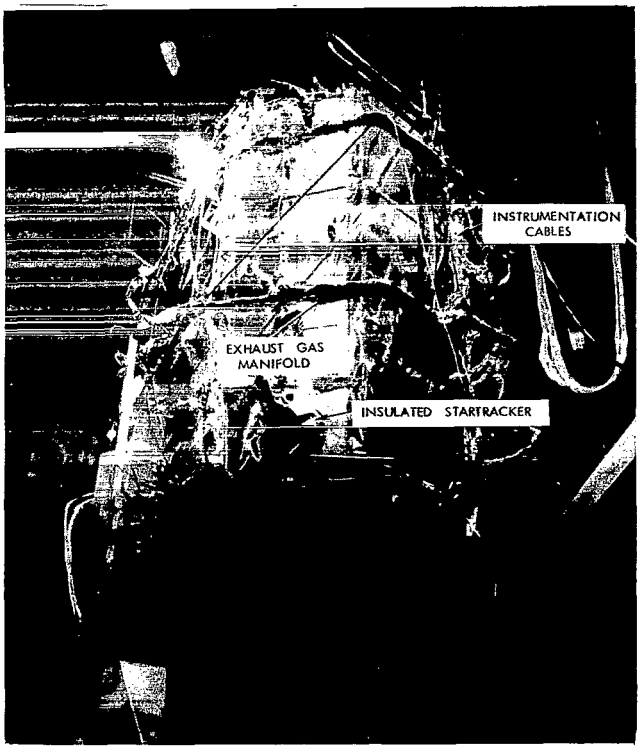

Figure 14—The flight spacecraft.

Early Thermal-Vacuum Test (ETV)

The ETV test of OAO 2 had several objectives in the following order of priority:

(1) To demonstrate proper systems operation and freedom from electromagnetic interference effects at temperature extremes that would, in most cases, equal qualification levels on a bay-by-bay basis.

(2) To demonstrate proper operation of the power subsystem under worst-case electrical-thermal conditions.

(3) To determine the heat leak from the experiments.

(4) To correlate flight spacecraft temperatures versus the thermal model for at least one common point.

(5) To determine the overall leak rate of the stabilization and control subsystem.

(6) To demonstrate that the Observatory did not have any high-voltage problems.

To meet the above objectives, a thermal test profile was designed, which took 13 calendar days exclusive of experiment optics warmup. The test profile had five parts:

(1) Simulation of orbital injection temperatures with the heater skins and cooling of equipment to steady state by a simulated initial stabilization flux profile, $\beta = 0°$.

(2) Placement of the Observatory in the coldest possible condition for all bays. [This was a fictitious condition, where an attempt was made to drive all bays to their lower acceptance limit for electromagnetic compatibility checks (EMC).]

(3) Following EMC checks, return of the Observatory to the $\beta = 0°$ flux mode and check of the power subsystem.

(4) Simulation of the sunbathing orientation, $\beta = 123°$, for additional power subsystem checks. (Enough time was allocated to achieve a thermal steady state also.)

(5) Placement of the Observatory in the hottest possible orientation for all bays to perform EMC checks.

In the test, the batteries and other power subsystem equipment performed satisfactorily at the expected flight temperature extremes. The batteries survived forced undervoltage and subsequent recharge without temperature problems. During the hot-case test phase, at a higher power level, the thermal control scheme proved adequate in holding the battery temperature below the upper limits.

Several test anomalies were uncovered:

(1) Due to expansion cooling through the pressure regulator, bays A-3 and E-3 experienced under-temperature conditions during prolonged firings of the high-thrust jets. No design changes were necessary, since this condition was not expected in flight.

(2) The tape recorder bay (A-5) violated its lower acceptance limit. This was caused by the incorrect wiring of the thermostatically controlled heater, an irregularity that gave a lower power rating.

(3) Several bays, including G-3 and G-4 (IBM units), sustained abnormally large temperature gradients. Since these did not affect electrical operation, design changes were not necessary.

(4) The thermostat for the SAO electronics heaters (bay E-4) was set incorrectly, causing the unit to run colder than desired. The thermostat was replaced.

(5) Though the experiments performed well, the measured heat leak was greater than predicted. As in the thermal model test, the problem was the radiation seal leak and the lack of prediction ability. The analytical model was revised and further comparisons were made in following tests.

Thermal-Vacuum Acceptance Test (LTV)

The LTV test had several objectives in the following order of priority:

(1) To demonstrate the flight acceptance of the OAO 2 by proper performance under those simulated space conditions met in the first 4 days of orbital operation, during the thermally stable aspect angles of $\beta = 45°$ and $\beta = 90°$ A, and during thermal cycling of equipment.

(2) To simulate near-orbital operation and to monitor the overall performance of the power subsystem.

(3) To provide ground simulation for training personnel in orbital operations.

The above objectives were met with a thermal test profile which lasted 14 calendar days excluding experiment optics warmup. The profile was as follows:

(1) Simulation of orbital injection temperatures with the heater skins, then simulation of fluxes incident on the OAO during the first 4 days of the Mission Operations Plan. (This meant four orbits at $\beta = 0°$, 39 orbits at $\beta = 123°$, then two more at $\beta = 0°$.)

(2) Achievement of a stable thermal point in the $\beta = 45°$ orientation.

(3) Achievement of a stable thermal point for $\beta = 90°$ with the A side in the sun.

(4) Thermal cycling of equipment by alternating $\beta = 90°$ A and $\beta = 90°$ E fluxes.

In general, the overall performance of the thermal subsystem was good. Design changes incorporated after the ETV test were effective. The steady state conditions during the ETV and LTV tests represented the full range of expected operating temperatures. In addition, a good deal of confidence was gained in the first 4 days of the Mission Operations Plan.

The major problems in the test were the excessively warm temperature level for the Alzak heater skins and the refusal of the batteries to accept charge in the cold condition. The hot-skin problem was not totally resolved (see "Summary of Thermal Test Problems"). The battery problem, on the other hand, was corrected by replacing the defective units.

It was judged that the skins contributed to warmer equipment temperatures and that design changes were not warranted in those bays that slightly exceeded their upper acceptance temperatures; namely, bays A-5, B-4, D-4, and F-4.

In the LTV test, several thermostats controlled bays a few degrees below the lower acceptance limit. The maximum out of tolerance condition was 3° to 4°C for the bore-sighted startracker. Since all equipment functioned well despite the out of tolerance condition, no attempt was made to change the thermostats.

The functional anomalies found in test are enumerated below:

(1) The tape recorder exhibited excessive error rates at cold conditions and was replaced with a flight spare.

(2) The flight thermistor on the voltage regulator converter failed and had to be replaced.

(3) The WEP stellar No. 4 telescope exhibited a loss of analog signal at cold temperatures. This problem had occurred in previous testing at the Observatory level and at the experiment level. The fault apparently had not been remedied by several modifications. Since the signal was redundant with a digital one, it was decided not to repair the fault.

ANALYTICAL SUPPORT

The test program analytical support was divided into several activities. These were—

(1) Verification, or modification, of the computer model used to generate flight predictions.

(2) Determination of the degree of test simulation.

(3) Determination of the level of confidence in the collected test data.

The major concern of the analytical support effort was the verification of the analytical model. This computer model (Reference 7), developed for OAO 2, consisted of approximately 300 isothermal nodes, which described the spacecraft main body and the various spacecraft appendages.

The digital program operated on the basic heat balance equation

$$T' = T + \frac{\Delta\tau}{mc_p}\left[\mathrm{QCONS} + \sum_{i\equiv 1}^{n}\left(\frac{kA}{x}\right)_i (T_i - T) + \sigma \sum_{j\equiv 1}^{m} (A\mathcal{F})_j (T_j^4 - T^4) - \sigma\epsilon A T^4\right],$$

where

T = node temperature at time τ,

T' = node temperature at time $\tau + \Delta\tau$,

mc_p = mass-specific heat product for the node,

QCONS = constant heat rate absorbed by the node,

$\sum_{i\equiv 1}^{n}\left(\frac{kA}{x}\right)_i (T_i - T)$ = heat conducted to the node from other nodes,

$\sigma \sum_{j\equiv 1}^{m} (A\mathcal{F})_j (T_j^4 - T^4)$ = heat radiated to the node from other nodes, and

$\sigma\epsilon A T^4$ = heat radiated to space by the node.

In an effort to validate* the computer model, the program was implemented to obtain steady state data before and after the three integrated thermal-vacuum tests. The amount of test prediction data allowed two different model verification techniques.

One approach, attempted after the thermal model test, was a matrix inversion technique used to calculate the electronic component couplings (to other components, to skin, and to structure).

The radiative couplings were computed from the experimental data by writing the heat balance relations for the nodes in question and then by solving the determinate system of linear algebraic equations that derive from using the appropriate number of test conditions. The sets of equations were written in the following form for any node i (Reference 8):

$$[P_{i,N}] = [\chi_{i-j,N}]\,[G_{i-j}],$$

where

$P_{i,N} \equiv$ power to node i for case N,

$\chi_{i-j,N} \equiv \sigma\,(T_i^4 - T_j^4)$, the potential difference from node i to node j for case N,

$G_{i-j} \equiv$ radiative coupling $(A\mathcal{F})_{i-j}$ between node i and node j,

$i,j \equiv$ node numbers, and

$N \equiv$ case number.

Thus, to solve for the radiative couplings G_{i-j}, the quantities required were the powers $P_{i,N}$, the driving force arrays $\chi_{i-j,N}$, and the nodal arrangement. The values of the power and the driving force arrays were obtained from test data.

Two support computer programs were combined to aid in solution of the equations. The first program provided a selection routine using the input (test) data to set up the power and driving force arrays required in the matrix solution. The second program, a matrix inversion subroutine, used the data output from the first program to solve the system of equations by use of pivoting and Gaussian elimination.

The effort was not totally successful, because several of the steady state conditions gave test data that were not sufficiently different to afford optimum mathematical solution, i.e., some test data did not produce linearly independent heat balance equations in every case. The technique, however, did reveal areas in the spacecraft computer model that required coupling changes.

*Validation of the computer model meant the adjustment of thermal couplings until the predicted temperatures agreed with test values.

The method ultimately followed was the standard technique, whereby the computer model coupling changes were based on engineering judgment. Sensitive couplings were varied after all integrated thermal-vacuum tests in order to bring test and predicted test temperatures into agreement. The results of the effort are given in Table 3.

Table 3—Nodal temperature summary.

Aspect angle	Spacecraft subdivision	Number of nodes	Percent of nodes within indicated temperature ranges					
			Predicted vs test values			Predicted vs flight values		
			0°-5° C	5°-10° C	over 10° C	0°-5° C	5°-10°C	over 10° C
β=123°	Structure	48	100	...	...	63	25	12
	Skins	56	24	46	30	100	...	...
	WEP	45	83	...	17	20	80	...
	SAO	51	50	17	33	...	...	...
	Components	51	72	23	5	97	3	...
β=45°	Structure	48	100	...	...			
	Skins	56	40	26	34			
	WEP	45	83	...	17			
	SAO	51	66	17	17			
	Components	51	65	30	5			
β=90°A	Structure	48	100	...	...			
	Skins	56	20	40	40			
	WEP	45	83	...	17			
	SAO	51	17	17	66			
	Components	51	67	21	12			

At the conclusion of the analytical model adjustment, flight temperature prediction bands were generated. Included in the computer inputs were tolerances on all thermophysical properties, on environmental inputs, and on power dissipation rates. The large variations in the input parameters resulted in a large temperature prediction band.

After the spacecraft was launched and the power dissipation rates were established for the steady state conditions of the first 650 orbits, a new set of nodal temperature predictions was obtained. The prediction-to-flight comparisons are also presented in Table 3.

In addition to verification of the analytical model, differences between test and space environments had to be established prior to the evaluation of the Observatory thermal design. This objective was met by determining the thermal inputs from the various test appendages and from the chamber walls to the spacecraft. These effects were then "subtracted" from the test results to reflect actual flight behavior.

The complement of the test appendages consisted of solar sensor stimulators, spacecraft holding fixtures, and piping to take the stability and control subsystem gases out of the chamber.

The thermal input from these test appendages took two forms:

$$Q = \sigma A F \epsilon \theta^4, \tag{1}$$

for those cases where only radiation effects were present, and

$$Q = Q_{\text{conducted}} + Q_{\text{radiated}}, \tag{2}$$

for those cases where both radiation and conduction were important.

Here,

Q = heat input,

σ = Stefan-Boltzmann constant,

A = radiating surface area,

F = form factor,

ϵ = emissivity of the surface, and

θ = temperature of the surface.

Since conduction and radiation terms in Equation 2 are interdependent, it was necessary to determine the temperature profile in a manner best discussed by Jakob (Reference 9). Thus,

$$KA' \frac{d^2\theta}{dx^2} = h_r \theta, \tag{3}$$

where

K = thermal conductivity,

A' = cross-sectional area for conduction, and

h_r = heat transfer coefficient for radiation.

The form factor F in Equation 1 was, in most cases, calculated by CONFAC (Reference 10). Solution of Equations 2 and 3 required that enough boundary conditions be available to calculate the constants of integration. The other factors, including the heat transfer coefficient for radiation, h_r, were easily determined once the form factor was computed for the appendage under analysis.

An analysis of the thermal influence of the spacecraft holding fixture was performed during the thermal model test by developing an electrical analog of the specially designed adiabatic spacecraft-chamber interface. The maximum energy loss from the Observatory was calculated to be 8 W.

The thermal exchange between the control system exhaust lines and the spacecraft skins was determined by developing a four-node computer program, which included the spacecraft skins, the chamber walls, and the exhaust system piping. The program, limited to first reflections only, determined the net flux error on all spacecraft skins to be ±6.6 W. (The low flux is a result of cooling and insulating the exhaust lines.)

The chamber wall infrared energy inputs to the spacecraft were determined for a single skin, by use of a radiosity network, and for the entire spacecraft, by a digital program that consisted of eight skin nodes and the chamber wall average temperature. The analysis was performed during the thermal model test with the solar simulator off. The calculated infrared energy absorbed by the spacecraft (282 Btu/hr) was assumed to be constant for the tests that followed.

Coincident with studies to determine the various test inputs to the spacecraft, a program was conducted to determine the accuracy of the collected test data. To begin, the accuracy of the readout equipment and collection system was determined by calibration against standard signals. In addition to the electrical checks, the tolerance bands about the various calculated parameters were determined, using a finite difference approach. For example, from the simple radiation equation $Q = \sigma A F \epsilon \theta^4$, the flux uncertainty ΔQ was determined from the relation

$$Q + \Delta Q = \sigma\,(A+\Delta A)\,(F+\Delta F)\,(\epsilon+\Delta\epsilon)\,(\theta+\Delta\theta)^4,$$

where all other uncertainties are known quantities. This technique was applied to all heat balance equations. The combination of error analysis and calibration of the collection system established a high level of confidence in the test monitoring.

FLIGHT RESULTS

The OAO 2 spacecraft was launched from the Eastern Test Range on December 7, 1968, at 0840 GMT. The spacecraft was initially stabilized with the aft end facing the sun ($\beta = 0°$). After four orbits it was reoriented to the sunbathing mode ($\beta = 123°$) for the next 39 orbits, while all systems were checked.

The date of the launch placed the Observatory in a 65% to 66% sun-time orbit. By the 43rd orbit, when the spacecraft was oriented for the first star pointing, the temperatures had stabilized and thus provided the first check on the spacecraft's thermal design.

For the first day, there was close agreement between the predicted and flight cooldown rates. Afterward, the comparison was not so good, because the flight power dissipations were 75 to 125 W higher than the predicted levels. The average structure temperature in flight was approximately 6° C higher than predicted after 100 hours in orbit (Reference 11).

Following this stable case, the Observatory operated alternately—one week with the sun on the D, E, and F sides, the next week with the sun on the A, B, and H sides—while the WEP and SAO experiment operations alternated also. This operating mode provided four more stable points: two at $\beta = 78°$ on the A side, and two at $\beta = 101°$ on the E side.

Neither of these aspects was tested, nor were predictions generated. These cases were investigated after the fact, by use of the correlated analytical model.

Computer runs were made for 65.2% sun-time orbits of $\beta = 123°$, $\gamma = 180°$; $\beta = 105°$, $\gamma = 180°$; and $\beta = 75°$, $\gamma = 180°$. (Environmental inputs to the spacecraft were computed for aspect angle increments of 15°. Thus, $\beta = 75°$ and 105° were approximations to actual flight aspects of $\beta = 78°$ and 101°.) The equipment power dissipations were re-evaluated to give the best flight estimates. Table 4 lists the flight and predicted equipment temperatures (Reference 11).

Table 4—Predicted versus flight component temperatures (°C).

Bay location of equipment	$\beta = 123°$		$\beta = 101°$		$\beta = 78°$	
	Flight	Predicted	Flight	Predicted	Flight	Predicted
A-2	- 4	- 4	-2	- 2	16	19
A-3	- 3	- 2	0	0	23	20
A-4	- 7	3	-3	4	23	24
A-5	7	7	5	7	9	7
B-2	- 5	- 3	-4	- 3	16	19
B-3	3	3	5	4	26	21
B-4	5	5	5	5	26	26
B-5	17	15	17	16	19	25
C-3	18	22	21	22	21	24
C-4	11	14	11	14	10	15
D-2	20	20	23	23	11	11
D-3	26	22	29	24	15	14
D-4	20	20	27	23	3	2
D-5	5	8	11	23	5	13
E-1	17	15	17	16	9	11
E-2	18	17	24	21	-5	-2
E-3	24	20	28	22	12	11
E-4	15	20	23	23	2	-1
E-5	5	6	18	25	11	14
F-2	18	20	21	23	6	6
F-3	21	21	24	23	2	7
F-4	22	20	28	23	6	3
F-5	40	36	41	37	27	31
G-3	27	24	28	23	18	23
G-4	33	33	35	33	31	33
H-2	- 8	- 8	-7	- 7	6	12
H-3	-12	-11	-9	-10	8	12
H-4	9	11	13	12	30	30
H-5	4	8	6	9	16	17

With the exception of bays A-4, D-5, and E-5, the predicted component temperatures for each bay fell within 6° C of their respective flight values. Bay A-4 was strongly dependent on the activities of the wide-band transmitter, particularly during dark-side operation ($\beta = 101°$). Since the transmitter was cycled, it was difficult to establish a steady state condition in bay A-4. Bays D-5 and E-5 were evaluated with bay D-5 equipment in an "on" rather than a "standby" mode. The predicted temperatures would have been closer to flight if the correct power levels had been used (2.7 W "on" as opposed to 1.7 W "standby") (Reference 11).

Comparison of structural temperature levels and gradients in flight (Reference 11) with those predicted and observed in test revealed the following:

(1) During E-side operation ($\beta = 101°$), the structural truss on this side near the forward end was 7° C warmer than predicted.

(2) During A-side operation ($\beta = 78°$), the structural truss near the aft end was 6° C warmer than predicted.

(3) The average structure temperature in flight was higher than predicted.

(4) The circumferential gradients were larger than expected.

The warm structural truss readings for both A and E side operations were caused by the location of the flight thermistors. Both were positioned near startracker mounting legs and sunshade hinge beams, which, when in sunlight, became an additional heat source to the truss thermistors. Moreover, since the truss line in sunlight was always warmer than predicted, there appeared to be a uniform heat input on that side. The increase in temperature along the truss was attributable to entrapped and absorbed solar energy in the cavities between the Alzak skins (Reference 11). This input was not simulated in test and was not included in predictions.

Though the average structure temperature exceeded predictions, there was no significant difference in equipment temperature levels. Since the flight structure temperature was the average of only eight thermistors, all located on either the A or E side of the spacecraft, a higher structure temperature was expected, for reasons discussed in the previous paragraph.

The WEP and SAO temperatures in flight showed close agreement with predictions. See Tables 5 and 6 (Reference 11).

More recently, the spacecraft was stabilized at $\beta = 123°$, 80% sun time, after almost 6 months of operation. Spacecraft temperatures were warmer in flight than for the $\beta = 123°$, 83% sun-time case run in the ETV test. The temperature differences were due to the fact that test conditions were based on nondegraded Alzak ($\alpha = 0.15$), whereas flight data indicated that the Alzak skins were degraded ($\alpha = 0.20$). The fact that both sunshades were closed in flight, in contrast to the test cryopanels, which were adjusted to simulate the open position, also contributed to these temperature differences.

Table 5—WEP flight temperatures (°C).

Module	β = 123°		β = 101°		β = 78°	
	Flight	Predicted	Flight	Predicted	Flight	Predicted
Nebular	-23	-28	-22	-26	-21	-21
Stellar 1	-18	-24	-18	-24	-19	-20
Stellar 2	-17	-24	-17	-23	-19	-18
Stellar 4	-19	-26	-19	-24	-17	-21
WEP structure	...	-17	-13	-17	-12	-16

Table 6—SAO flight temperatures (°C).

Component	β = 78°	
	Flight	Predicted
Uvicon 3	-23	-33
Uvicon 4	-24	-39
Telescope 2	-34	-38
Telescope 4	-38	-41
Cal lamp 2	-42	-48
Cal lamp 4	-48	-51

On the whole, the spacecraft thermal behavior was close to that predicted by the analytical model, as verified by test results. The flight data showed that all monitored temperatures fell within acceptance values, thus indicating satisfactory thermal performance.

SUMMARY OF THERMAL TEST PROBLEMS

The problems encountered during the OAO 2 development program were of two varieties, chamber related and spacecraft related. Though a detailed discussion of all problems was beyond the scope of this paper, certain anomalies judged to be of general interest are presented here. They portray some of the sensitive areas of large-scale observatory testing and heater skin simulation.

Chamber Related Problems

Though chamber problems affected spacecraft temperatures, system errors associated with solar simulation and temperature measurement were relatively independent of the test object.

Errors associated with solar simulation were attributed to the fact that a test object in the SES views Cassegrain elements (parabolas, hyperbolas), relay lenses, and the chamber dome directly. A test was performed during the OAO program with the chamber lamps on to determine the solar simulator emissions in the spectral range of 2.9-29.3 μ. The infrared input was found to include a diffuse component (direct emission from the parabolas, relay lenses, and the dome) and a collimated component (energy transmitted through the optical train). The total magnitude of this input, dependent on the distance between source and test article, varied from 4.6 to 13.5 mW/cm^2 (Reference 12). This input constituted an appreciable source of error for coatings like Alzak with a high absorptance in the infrared region of the electromagnetic spectrum.

Attempts to measure the infrared radiation from the dome, when the simulator was off, failed since the measuring instruments were not sensitive enough and did not view enough of the dome surface. It is noted, however, that the support analysis indicated that the energy input was negligible with respect to the total spacecraft input.

Monitoring errors, associated with the inability of the commonly used detectors (solar cells and integrating spheres) to provide narrow spectral band information, also caused significant problems for the Alzak skins, which have several absorptance peaks.

Another source of test errors was that inherent in the temperature measurement system. There were 450 thermocouples and 100 thermistors in a typical OAO spacecraft test. During the test, an output signal from the temperature sensor was amplified and sent to a computer in the Data Central complex. The computer then furnished a conversion reading in degrees Celsius for that sensor location. The conversion errors inherent in Data Central were estimated to be $\pm 1^\circ$ C for both thermocouples and thermistors.*

For copper-constantan thermocouples, used exclusively in test, the normal temperature range is -200° to $+210^\circ$ C. A study conducted at GSFC† revealed that the average variation for several different types and gauges of copper-constantan thermocouples changed with the temperature level. At temperatures of -195° C, the deviation was $\pm 6.4^\circ$C; at -77°C, it was $\pm 2.7^\circ$C; at around 0°C, it was $\pm 0.4^\circ$C; at 25°C, it was $\pm 0.2^\circ$C; and at 100°C, it was $\pm 0.8^\circ$C. The thermistors used in test were YSI precise thermistors. The manufacturer's specifications gave tolerances of $\pm 0.45^\circ$C for the temperature range -40° to $+120^\circ$C and tolerances of $\pm 1^\circ$C for the temperature interval -80° to $+150^\circ$C.

The temperature sensor errors presented above showed that, depending on the temperature range considered, the uncertainties could be significant. Since most of the OAO spacecraft thermal sensors monitored temperatures in the range -82° to $+50^\circ$ C, the maximum expected error was $\pm 3^\circ$C.

*Scott, C., Electronics Test Branch, Goddard Space Flight Center, private communication, June 1969.

†Wilson, M., and Foy, C., "Accuracy of Temperature Measurements Using Building Seven Data Collection System," Electronics Test Branch, Goddard Space Flight Center, unpublished report, Jan. 1964.

Spacecraft Related Problems

This second category of problems was unique to the test object. The most significant problems experienced during the OAO test program are listed and then discussed in detail below.

(1) The Alzak heater skins ran hotter than expected in all tests. Further, Alzak properties varied with temperature and initially showed large degradation rates when exposed to the mercury-xenon lamps of the SES.

(2) The startracker test-to-predicted temperature difference was large.

(3) The measured experiment heat leak exceeded predictions.

(4) Verification of the comprehensive model was complicated by the limited number of nodes available and by difficulty in estimating couplings through multilayered superinsulation.

(5) Experiment optical performance could not be measured during integrated thermal-vacuum testing.

(6) Contamination of the spacecraft had to be prevented.

Alzak Heater Skin Temperature Anomaly

During the thermal model test, the early thermal-vacuum test, and the flight acceptance test, the Alzak heater skins consistently ran hotter than the predicted temperatures. The anomaly was greater for both flight unit tests than for the thermal model. Approximately 4% of the heater skin temperatures were greater than 20°C above predictions in all three tests, and approximately 30% of the nodes were greater than 10° C above predictions.

The six sources of error (all in the hot direction) are discussed below.

Lack of Total Heater Skin Coverage

The Nichrome heaters covered only 95% of the total flat surface of the test skin; typically, the perimeter was not covered. Thus, the total orbital average flux was input to an area smaller than in flight. The result was an increase in the flux density in the center of the skin, where the temperature sensor was positioned.

Skin Edge Effects

The Alzak skins had a 1 in. lip around the periphery to afford structural rigidity. This edge, which accounted for approximately 12% of the total area, was not heated. The result again was an increase in the flux density over that area of the skin which the heater did cover.

Test instrumentation cable bundles, running along the outside of the Observatory between adjacent skins on four of the eight truss lines, caused a blockage of the skins to the wall. Since the cable bundle diameters were variable, and since all skins were not involved, the magnitude of the effect was not estimated.

Effects of Skin and Heat Sink Temperature Gradients

The Alzak heater skins, nominally 10 mils thick, sustained a lateral gradient during test. During the LTV test, a gradient of 7° C was measured from the center of the skin to the edge.

Equipment, mounted on the inboard heat sink behind the skins and in an area near the center of the skins, compounded the error by an amount dependent on the particular heat dissipation rate of the bay in question. See Figure 6 for heat sink, equipment, and skin arrangement.

A gradient through the skin was also experienced because of the test heater buildup, which included Alzak, a double layer of Fiberglas, and a Nichrome heater (Figure 15).

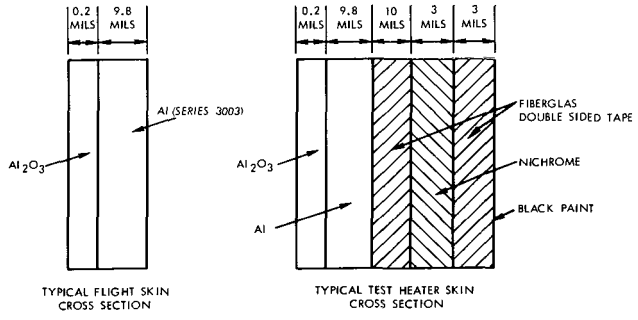

Figure 15—Flight and heater skin construction.

Extraneous Energy Effects

Since the SES effective sink temperature was found to be -160° C, and since the chamber walls are not totally black, extraneous emitted and reflected inputs to the spacecraft were present.

The magnitude of the direct energy input from the chamber with the lamps off was determined to be negligible in the integrating sphere calibration test phase (see "Test Results," above).

Diffuse emissions from the spacecraft were reflected back to the spacecraft in direct proportion both to the wall reflectance and to the configuration factor between the walls and test object. The SES chamber reflectance was 6% and the configuration factor (walls-to-spacecraft) was 0.06. This effect resulted in approximately 10 W of reflected energy being absorbed by the skins out of a 3000 W input to the skins.

Test Configuration Effects

All errors discussed thus far were common to both the thermal model and the flight units. The major difference between units was that of test configuration. The thermal model had no appendages except for the H-6 startracker minaret. The flight units, on the other hand, were configured with a manifold to remove gas from the high- and low-thrust jets, with GN_2 fill and dump lines, with optical stimuli for the various sensors, and with collimators over all startrackers. Test hardware either provided an additional source

of infrared energy to the local skin or blocked radiant energy leaving the skin. Several tests and support analyses were performed during the acceptance test to define this effect.

Effects of Skin Property Variation

It is known that the emittance of Alzak varies with anodize thickness and temperature (References 13-16,*). The effect of lowering the emissivity was to reduce the heat rejection capability of an Alzak skin, with a corresponding increase in temperature. To compound the uncertainty, the absorptivity of Alzak varies with time, temperature, test lamp spectrum and intensity, and *in situ* effects (References 17-19,†).

Two general methods exist for obtaining thermophysical properties of materials, the photometric method and the solar-vacuum technique. The former is an optical method, which can be performed in air or in a vacuum. It is limited, however, because test specimens have to be moved out of the intensity source while measurements are in progress. Also, thermophysical properties of large test items can only be measured locally by this method, since only a small area can be exposed to the photometric instrument. For these reasons, the solar-vacuum measuring technique was employed to obtain α and ϵ information on the OAO Alzak heater skins.

Another measurement problem occurs when thermophysical behavior of materials must be determined for long periods of time in the space environment. Smith and Lee (Reference 20) indicate that to obtain reliable data for changes in absorptivity "both the magnitude and spectral distribution of the irradiance on the surface should closely approximate that of the sun" in the same wavelength interval. "This conclusion questions the reliability of data obtained in accelerated solar radiation testing where, to save time, it is assumed that the same test results for $\Delta\alpha$ can be obtained by substituting high-intensity ultraviolet source irradiance for irradiation time."

In summary, the temperature errors resulting from all the effects discussed above are presented in Table 7. The first four error categories could logically account for the skins' running warmer than predictions by as much as 10° C. From the table, it was also possible for the skins to run slightly warmer yet during flight unit testing. The average of all skin errors in the thermal model test was 4° to 9° C; the average error in the flight unit tests was 6° to 11° C. Thus, a configuration error of 2° C was plausible.

Since anomalies of 20° to 25° C occurred in 4% of all cases, factors other than those discussed above must be considered. Other considerations included very low emittance effects, the lifting off of skin heaters (thus causing localized hot spots at the points of measurement), larger inputs from components to skins, and abnormally large localized inputs from test hardware.

*Holley, J., Thermophysics Branch, Goddard Space Flight Center, unpublished laboratory data, Aug. 1968.

†Heaney, J., "Alzak Degradation Studies," Thermophysics Branch, Goddard Space Flight Center, unpublished report, Sept. 1967.

Table 7—Factors influencing test skin temperatures.

Sources of error	Error (° C)
Lack of total heater skin coverage	2° (low flux skin), 3° (high flux skin)
Edge effects	2° (low flux skin), 3° (high flux skin)
Skin and heat sink gradients	3° (estimate)
Extraneous energies:	
Chamber emitted	1°
Chamber reflected	Negligible
Test configuration effects:	
Thermal inputs from appendages	1° (estimate)
Blockage	1° to 3°
Skin property variation	3.5° (low flux skin), 1° (high flux skin)

An investigation program to study the impact of each of the above considerations was realized to be a larger effort than either time or available manpower would allow. For these reasons, the effort was not continued prior to OAO 2 flight.

Startracker Problem

The startrackers were controlled to analytically predicted temperatures for the entire integrated spacecraft test program, except for two brief solar simulation tests, performed on a prototype unit, during the thermal model test. In this test, several mercury-xenon solar modules irradiated the startracker minaret and thermal cover in an effort to determine the degradation rate of the exposed coating (Pyromark white paint) and to establish the temperature level of the telescope and housing.

Coincident with the testing, an analog computer program (Reference 21) was developed and test temperature predictions were generated. The prediction-to-test temperature difference was small for the eclipse cases; a large difference, however, existed for the case where the prototype startracker was exposed to chamber solar irradiation.

The test problem discussed above was associated with a prototype gimbaled tracker, which consisted of optics, telescope housing, sunshield, and minaret (see Figure 13). All other gimbaled startrackers had their minarets replaced with an insulating blanket, and test heaters (for temperature control) were positioned on the electronics baseplate. The purpose of the blanket was to provide a light-tight arrangement so that, by means of a special stimulator, the startracker signal acquisition capability could be monitored. The configuration, however, negated the possibility of performing thermal balance tests on the units.

From the results given in Table 1, it was seen that for the no-solar baseplate heater test conditions, the telescope housing test-to-prediction temperature comparisons were in good agreement. It was also seen that, in both solar cases, the housing temperatures were higher than predicted and were still rising when the test was terminated (indicated by arrows in Table 1). The problem was caused by errors either in the analog program or in the monitored test inputs. The test errors could be associated either with environmental inputs or with inaccuracies in solar simulation.

According to a recent paper (Reference 22), the inaccuracies due to solar simulation monitoring can be held within ±3% to ±5%, a value much below that required to explain the differences between the experimental and theoretical results for the startracker.

Though spectral measurements in a test chamber are difficult and data lacking, spectral information was available for single mercury-xenon lamps in air. With these data and a digital program, the effective absorptivity of Pyromark paint was determined for the chamber lamp spectrum and compared against the absorptivity for the Johnson sun. The calculated absorptivity ($\alpha = 0.3$) for freshly painted undegraded Pyromark was put into the analog model.

With the care exercised in the test, it was concluded that the basic problem was explained by both the degraded condition of the Pyromark and by the model arrangement as discussed below.

The original analog model (Reference 21), describing the six critical nodes, was complicated by several factors:

(1) The minaret was oddly shaped, which made the solar absorbed energy inputs difficult to model.

(2) The flux transfer from the thermal cover (sunshield) and the telescope housing was accomplished through a multilayered insulation blanket, and thus the effective conductance had to be estimated.

(3) Reflections off the minaret to the sunshield and spacecraft skins were known to exist but could not be modeled accurately.

The analytical model was revised (Figure 16) and the effective thermophysical properties were changed (Reference 23). The modified program was expanded to seven nodes by separating the telescope and telescope cover into single nodes. The effective couplings were recalculated for the insulation blankets between the telescope and the telescope thermal cover and between the housing and the housing thermal cover. The program was then rerun, with the result that agreement between test (46° C) and prediction (38° C) was considered acceptable.

Experiment Heat Leak

Two 4 ft diameter apertures and positionable sunshades, which protected the experiments from viewing the sun directly, were located on the forward and aft ends of the Observatory. When the experiments were operating and the sunshades were open,

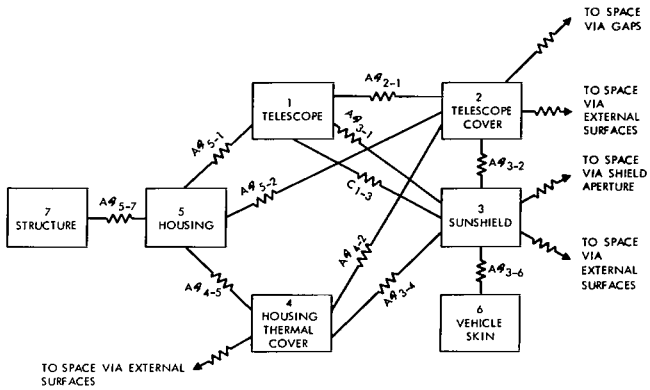

Figure 16—Nodal network for the OAO 2 startrackers.

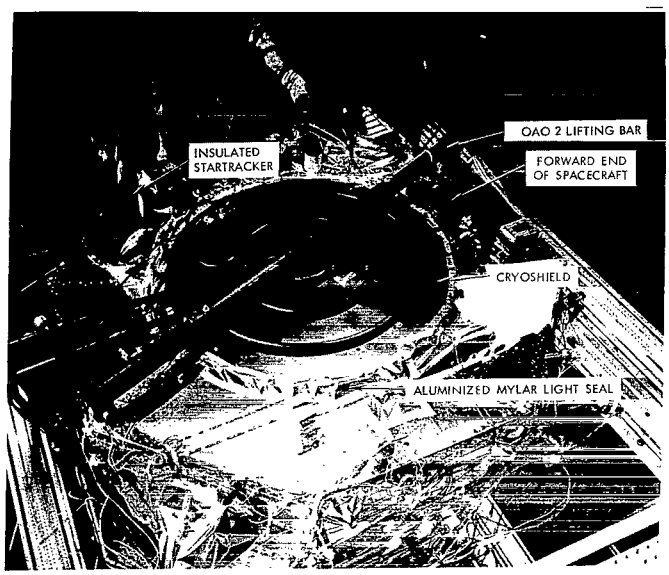

Figure 17—OAO 2 experiment cryopanel.

a spacecraft thermal loss, equal to approximately one-half the spacecraft cooling bay* emitted energy, was prevalent.

Since the thermal balance of the spacecraft was critical to flight mission success, the experiment heat leak had to be accurately measured in test. Heat-leak monitoring was accomplished by calibrated cryopanels in the configuration shown in Figures 17 and 18. It is noted that the 47 in. diameter black cryopanel arrangement also was used to simulate the environmental aperture fluxes.

The cryopanel calibration determined the heat input required to reach a certain stabilization temperature. A temperature-heat input curve was thus developed over the entire expected test range. In test, the difference between the heater input and the power to reach the cryopanel temperature was a measure of the cavity losses.

A radiosity network was developed to study the cryopanel-experiment interchange for the given test configuration. A 59-node digital program (Reference 24) was employed to investigate the thermal exchange between the WEP and its experiment aperture and sunshade, as well as that between the SAO and its experiment aperture and sunshade in flight configuration.

The thermal network between each cryopanel and experiment took into account the cryopanel emitted energy, the experiment emitted energy, and the experiment emitted enery that was reflected off the cryopanel. In the development of the radiosity analysis, two assumptions were made:

(1) The experiment could be approximated by a flat plate. (This is close to the actual configuration; each experiment has a flat surface with small light apertures facing the cryopanel.)

*The cooling bays (C-1, C-2, C-6, G-1, G-2, G-5, and G-6) are nonequipment bays with the insulation removed from the structure.

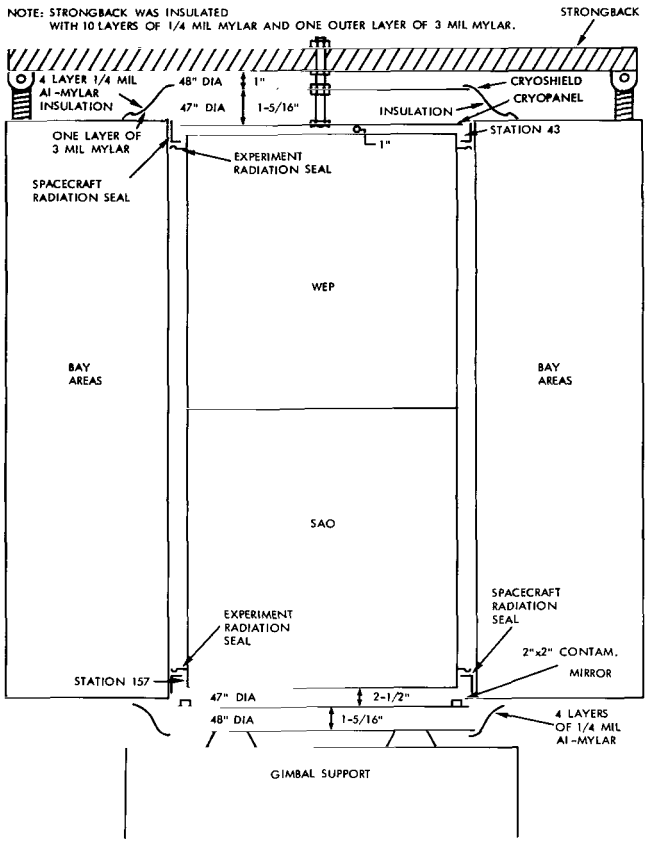

Figure 18—Experiment cryopanel details.

(2) The experiments were isothermal. (Test results confirmed that the temperatures were reasonably uniform.)

The analysis further required that the experiment temperatures be known quantities. Since these temperatures were not known before test, the radiosity analysis was run parametrically over the expected temperature range. The resultant difference in the heat leak was found to be small over the range chosen. A weakness in the study was the modeling omission of the light seals located in the experiment tube between the experiment and the structure.

The 59-node digital program treated the direct environmental inputs, the sunshade emitted energy to the aperture and space, and the specularly reflected energies from the spacecraft to the sunshade. The purpose of the program was to determine the effective cryopanel temperature necessary to simulate the space environmental fluxes. These effective cryopanel temperatures were determined and found to vary across the aperture. The maximum gradient was calculated to be 15° C for the hottest case. Unfortunately, the cryopanels could not be zone-temperature controlled, but rather were driven to a temperature corresponding to an average flux. Difficulties in this phase, then, were caused by the fact that specular reflections off the sunshade were not considered, and the cryopanel temperature was constant over the aperture.

Comparison of test to predicted losses (Table 8) revealed that the predicted losses were always smaller than the measured. While the percent differences between the two were large, the absolute value was small in comparison to the overall spacecraft heat balance. During the test program, the fact that the spacecraft computer program seemed able to predict the structure temperatures negated the need for further refinement of the auxiliary program developed for studying the experiment cryopanel arrangement. Flight results, indicating the lack of prediction ability of structure temperatures, caused a reinvestigation. This area is undergoing detailed analysis for the next OAO flight.

Differences between measured losses from the thermal model and from the late thermal-vacuum test were attributed to the fact that the light and radiation seal coatings were changed from Alzak to low emissivity tape (see Tables 2 and 8).

Table 8—Experiment heat leak comparison for the LTV test.

Aspect angle β	Experiment	Heat leak (W)	
		Measured	Predicted
90° A	WEP	23	11
	SAO	35	26
45°	WEP	31	18
	SAO	34	26

Deficiencies in Lumped Parameter Method and Problems in Verifying the Computer Program.

The mathematical modeling of a spacecraft is limited by several factors:

(1) Core size of the computer.

(2) Time available to develop the model.

(3) Ability to reduce large amounts of output data from the model.

(4) Ability to modify the program to bring test and predicted results into agreement.

For the OAO, the electronic components and their respective heat sinks in most equipment bays were grouped into one node. This "lumped parameter" approach was based on the assumption that the components in each individual bay would run at nearly isothermal temperatures.

During the various tests, thermocouples were mounted on components to check this assumption by measuring the various bay gradients. The largest minimum-to-maximum temperature gradient was found in the final acceptance test to be approximately 20°C for bay A-2. The majority of bays experienced a much smaller gradient.

The problem associated with large gradients across lumped parameter nodes commonly manifests itself in problems associated with verifying the analytical model. Two questions arise in this regard:

(1) Where should the test instrumentation be located?

(2) What type of averaging is necessary to determine the comparative test temperature?

The problem of instrumentation placement is solved by default. The location is decided before the test and is often dictated by the data collection facilities.

The type of averaging necessary to obtain the proper comparison temperature is more difficult. To begin, average temperatures are relatively meaningless unless a

tolerance band can be applied to the average. This usually requires adding more instrumentation than can be accommodated, so that maximum and minimum bay temperatures can be determined. In addition, the method of averaging raises the question as to whether area weighting or mass weighting of temperatures should be followed. For small heavy packages, mass-weighting appears to be the approach; for light large boxes, the area-weighting technique should be employed.

For the OAO, the problem was resolved either by increasing the number of nodes or by measuring the maximum gradient in each bay and imposing a tolerance band about the prediction.

In addition to the previous discussion, the problem of model verification is also greatly affected by the number of nodes and couplings. For a model the size of OAO, with 300 nodes and approximately 1700 couplings, the approach was to isolate the areas of large test-to-prediction differences and reevaluate the couplings to obtain closer agreement between prediction and test. Obviously, the more nodes, the more difficult the adjustment of the model. Further, the more nodes a mathematical model contains, the more data must be compared with test results.

The ideal approach to model verification appears to be computerization of the effort. The comparison and tabulation of test-to-prediction temperatures at GSFC's SES facility is presently automated, with the adjustment of couplings still handled manually. Approaches such as the matrix inversion technique, described earlier, are being studied and will be automated when development is completed.

Lack of Ability to Measure Optical Performance

As mentioned previously, one of the primary objectives of Observatory testing was functional demonstration at thermal extremes. For the OAO 2 test program, functional demonstration consisted of a thorough check of all electrical, electromechanical, and mechanical systems. Optical checks, i.e., stimulation of the WEP and SAO through their optical trains, could not be accomplished in the integrated spacecraft tests. Optical performance and calibration tests were performed on both experiments early in the OAO 2 history. Extremely tight launch schedules precluded calibration after thermal-vacuum acceptance. Additionally, because of the amount of Observatory tear-down and reintegration associated with a calibration effort, calibration of the experiment optics was not feasible. A GSFC test goal is testing of the flight configuration under acceptance levels, then flying with as little perturbation to this configuration as possible.

The topic of thermal-vacuum optical testing of diffraction-limited ultraviolet telescopes is the subject of a separate study (Reference 22). The scope of such testing can vary widely. It can take the forms of optical alignment checks, single point calibration, mirror figure accuracy checks, and even full-scale calibration. Suffice it to say here, the lack of an optical test under realistic orbital thermal profiles, as close to the launch as possible, presents the following risks:

(1) Failure to discover optical effects associated with element distortions caused by realistic temperature gradients.

(2) Failure to discover particulate and/or molecular contamination of the optics.

(3) Failure to reveal possible calibration shifts.

(4) Failure to uncover problems associated with degradation of the optics.

The OAO experimenter attempted to minimize the risk by employing in-orbit focusing and calibration schemes.

Contamination

During Observatory testing, several contamination problems arose. The problems encountered were from both particulate and molecular contamination.

Particulate Contamination

The potential for particulate contamination of the Observatory arose during the Observatory load and unload, when the chamber contamination barrier was disrupted. To prevent this form of contamination from occurring, the Observatory was wrapped in a polyethylene bag and purged with gaseous nitrogen. Great care was also taken to insure that the test facility was clean of particulate contamination by first washing the chamber with Freon TF and then by maintaining a flow of clean, dry air through the chamber.

Molecular Contamination

Because the OAO contained two optical telescopes, it was extremely important that every precaution be taken to minimize the potential for molecular contamination. This contamination could arise from any backstreaming of the oils in the chamber pumping system, from chamber outgassing, or from outgassing of the Observatory itself. To combat molecular contamination, the chamber facility underwent a great deal of pre-testing for sources of contamination and an extensive bakeout at 50°C.

During both Observatory tests (ETV and LTV), molecular-type contamination was found in the Observatory. Infrared spectroscopic examination of the residues indicated the presence of phthalate esters, hydrocarbons, and di-methyl silicones on the SAO cryopanel and WEP aluminized Mylar seal. An infrared analysis of "wipes" taken in approximately 50% of the spacecraft bays showed the presence of all the above contaminants but did not indicate whether the components acted as sources or receivers of the contaminant. A quartz crystal microbalance, which detects condensable material by natural frequency changes, and residual gas analyses indicated negligible contamination. This result implied that, even though the contaminants were present, they were not in sufficient quantity to contaminate the entire chamber. Thus, the contamination mechanism was due to a local evaporation from a relatively warm surface followed by a recondensation on a relatively cooler surface. It was therefore obvious that the contaminants

emanated from within the Observatory. Contamination of the experiment optics was prevented during test by controlling the temperature difference between the optics and the cryopanels. The cryopanels were maintained at least 20° C below the telescope optics.

CONCLUDING REMARKS

Though the heater skin test approach was dictated in part by facility problems, it should not be construed as a test program compromise. As evidenced by the successful flight, the technique must be considered as more than adequate. It is pointed out, however, that the method is neither a panacea nor a final resort. Heater skin testing is an acceptable and valid approach, but it must be performed with full knowledge of its limitations, which can only be determined by detailed calibration tests and supporting thermal analyses.

Another questionable area is the adequacy of present simulation systems in testing the more sophisticated satellites. As an example, the inability to test the optical characteristics of the OAO 2 under a thermal-vacuum exposure caused serious concern throughout the development program. Further, the calibration techniques commonly employed require more development of the chamber infrared narrow-band spectrum information to firmly establish the test reference plane.

The last significant item concerns itself with the fact that the testing community must redirect some of its efforts to the analytical functions necessary to sustain major programs. In this regard, additional analyses are required to better define and understand the various chamber errors and their impact on the test results.

Goddard Space Flight Center
National Aeronautics and Space Administration
Greenbelt, Maryland, December 15, 1969
831-31-25-01-51

REFERENCES

1. Ziemer, R. R., and Kupperian, J. E., Jr., "The Mission of the Orbiting Astronomical Observatory," NASA SP-30, Mar. 1963, pp. 45-51.

2. Hemmerdinger, L. H., "Thermal Design of the Orbiting Astronomical Observatory." AIAA Journal, Vol. 1, No. 5, Sept. 1964.

3. Mengers, D., "Orbital Mechanics Analysis for OAO Heat Flux Studies," Thermodynamics Technical Memorandum No. 252-5, Grumman Aerospace Corp., Bethpage, New York, Mar. 3, 1967.

4. Young, E., "OAO Testing in the Space Environmental Simulator," U.S. Government Memorandum, Thermodynamics Branch, Goddard Space Flight Center, Nov. 1966.

5. Marshburn, J. P., "Orbiting Astronomical Observatory, Test Program, Calibration Procedure for SES Optics and Black Ball," Thermodynamics Branch, Goddard Space Flight Center, Aug. 1967.

6. Wagner, C. A., "Analysis of Simulation Errors in a Thermal-Vacuum Environment." U.S. Government Memorandum, Thermodynamics Branch, Goddard Space Flight Center, Aug. 1968.

7. Bartilucci, A., and Wimpfheimer, F., "The Steady State Temperature Distribution by Numerical Integration of a 3-Dimensional Object by Conduction, Convection, and Radiation, Deck No. SS 70150-K." Memorandum Report PM-001-36, Thermo and Propulsion Department, Grumman Aerospace Corp., Bethpage, New York, Sept. 1963.

8. "OAO Thermal Model Test Report." Thermodynamics Branch, Goddard Space Flight Center, Feb. 1968, pp. 120-124.

9. Jakob, M., "Heat Transfer," Vol. 1, New York: John Wiley & Sons, Inc., 1949.

10. Toups, K., "A General Computer Program for the Determination of Radiant-Interchange Configuration and Form Factors—CONFAC II," SID65-1043-2, North American Aviation, Inc., Oct. 1965.

11. "OAO-A2 Thirty Day Flight Evaluation Report," Vol. 2, Grumman Aerospace Corp., Bethpage, New York, Apr. 1969.

12. Rogers, J. F., "Infrared Spectral Irradiance Measurements on a Space Environment Simulator," Master's thesis, Catholic University of America, July 1968.

13. Caren, R. P., "Low Temperature Emittance Determinations." Palo Alto Research Laboratory, Lockheed Missiles & Space Co., Palo Alto, California.

14. Sadler, R., and Johanson, N., "Evaluation of Alzak Emittance Using Anodize Thickness Measurements." OAO Project Memorandum No. 64-121, Grumman Aerospace Corp., Bethpage, New York, Dec. 1964.

15. Hass, G., Ramsey, J. B., Triolo, J. J., and Albright, H. T., "Solar Absorptance and Thermal Emittance of Aluminum Coated with Surface Films of Evaporated Aluminum Oxide," Progress in Astronautics and Aeronautics, Vol. 18, New York: Academic Press, 1965.

16. Sadler, R., and Hemmerdinger, L., "Alzak Emittance Test in 4'x8' Vacuum Chamber on 7-21-64," OAO Project Memorandum No. 64-081, Grumman Aerospace Corp. Bethpage, New York, Oct. 1964.

17. Sadler, R., and Johanson, N., "Thermal Crazing of Alzak," OAO Project Memorandum No. 65-036, Grumman Aerospace Corp., Bethpage, New York, April 1965.

18. Hass, G., Drummeter, L. F., Jr., and Schach, M., "Temperature Stabilization of Highly Reflecting Spherical Satellites," J. Opt. Soc. Am., Vol. 49, No. 9, Sept. 1959, pp. 918-924.

19. Hemmerdinger, L., "In situ Ultra-Violet Degradation of OAO Alzak at TRW—Preliminary Report." Thermal Lab Memorandum TLM-67-18, Grumman Aerospace Corp., Bethpage, New York, Aug. 1967.

20. Smith, A. M., and Lee, A.Y., "An Analytical Study of A Solar Degradation Model for Thermal Control Materials and Some Ramifications for Accelerated Solar Radiation Testing." Paper No. 68-780, AIAA Third Thermophysics Conference, Los Angeles, California, June 24-26, 1968.

21. Latour, A., and Kelley, M., "Thermal Performance of OAO Star Trackers." PIR-4T74-126, General Electric Missile and Space Division, Philadelphia, Pennsylvania, Aug. 1967.

22. Maurer, H., "Thermal Simulation Systems." To be published in Proceedings of Workshop on Optical Telescope Technology, Huntsville, Alabama, Apr. 1969.

23. Karhan, B., "Thermal Analysis: OAO Startrackers." General Electric Missile and Space Division, Philadelphia, Pennsylvania, Apr. 1968.

24. Thermal Analysis of the University of Wisconsin Experiment Package/Smithsonian Astrophysical Observatory Experiment." Final Report, Arthur D. Little, Inc., Cambridge, Massachusetts, Mar. 1969.

"The aeronautical and space activities of the United States shall be conducted so as to contribute . . . to the expansion of human knowledge of phenomena in the atmosphere and space. The Administration shall provide for the widest practicable and appropriate dissemination of information concerning its activities and the results thereof."

—NATIONAL AERONAUTICS AND SPACE ACT OF 1958

NASA SCIENTIFIC AND TECHNICAL PUBLICATIONS

TECHNICAL REPORTS: Scientific and technical information considered important, complete, and a lasting contribution to existing knowledge.

TECHNICAL NOTES: Information less broad in scope but nevertheless of importance as a contribution to existing knowledge.

TECHNICAL MEMORANDUMS: Information receiving limited distribution because of preliminary data, security classification, or other reasons.

CONTRACTOR REPORTS: Scientific and technical information generated under a NASA contract or grant and considered an important contribution to existing knowledge.

TECHNICAL TRANSLATIONS: Information published in a foreign language considered to merit NASA distribution in English.

SPECIAL PUBLICATIONS: Information derived from or of value to NASA activities. Publications include conference proceedings, monographs, data compilations, handbooks, sourcebooks, and special bibliographies.

TECHNOLOGY UTILIZATION PUBLICATIONS: Information on technology used by NASA that may be of particular interest in commercial and other non-aerospace applications. Publications include Tech Briefs, Technology Utilization Reports and Notes, and Technology Surveys.

Details on the availability of these publications may be obtained from:

SCIENTIFIC AND TECHNICAL INFORMATION DIVISION

NATIONAL AERONAUTICS AND SPACE ADMINISTRATION

Washington, D.C. 20546